NEURAL NETWORK-BASED PARAMETER ESTIMATION OF A LABOUR MARKET AGENT-BASED MODEL

TO BE PRESENTED AT THE 6TH WORLD CONFERENCE ON COMPLEX SYSTEMS (WCCS 2026)

M Lopes Alves
Department of Computer Science
Institute of New Economic Thinking
University of Oxford
Oxford, UK
alves.ml@cs.ox.ac.uk

Joel Dyer
Department of Computer Science
Institute of New Economic Thinking
University of Oxford
Oxford, UK

Doyne Farmer
Department of Computer Science
Institute of New Economic Thinking
University of Oxford
Oxford, UK

Michael Wooldridge
Department of Computer Science
University of Oxford
Oxford, UK

Anisoara Calinescu
Department of Computer Science
Institute of New Economic Thinking
University of Oxford
Oxford, UK

ABSTRACT

Agent-based modelling (ABM) is a widespread approach to simulate complex systems. Advancements in computational processing and storage have facilitated the adoption of ABMs across many fields; however, ABMs face challenges that limit their use as decision-support tools. A significant issue is parameter estimation in large-scale ABMs, particularly due to computational constraints on exploring the parameter space. This study evaluates a state-of-the-art simulation-based inference (SBI) framework that uses neural networks (NN) for parameter estimation. This framework is applied to an established labour market ABM based on job transition networks. The ABM is initiated with synthetic datasets and the real U.S. labour market. Next, we compare the effectiveness of summary statistics derived from a list of statistical measures with that learned by an embedded NN. The results demonstrate that the NN-based approach recovers the original parameters when evaluating posterior distributions across various dataset scales and improves efficiency compared to traditional Bayesian methods.

Agent-based modelling (ABM) is a computational methodology widely used to simplify the representation of the real world through abstraction and reductionism while focusing on specific tasks or phenomena Jackson et al. [2017]. ABMs have been particularly valuable in economic research due to their ability to simulate diverse scenarios beyond the constraints of traditional models that often rely on oversimplified assumptions — such as perfect rationality and equilibrium. In labour markets specifically, ABMs have contributed to clarifying how markets are shaped, constantly changing, and respond to shocks such as the economic impacts of social distancing interventions during the COVID-19 pandemic Silva et al. [2020].

Despite their potential use, ABMs face a significant issue in parameter estimation. ABM parameters, defined as $\boldsymbol{\theta}$, are typically distributed across a large parameter space, making their comprehensive exploration challenging. This study addresses this challenge by employing a state-of-the-art black-box simulation-based inference (SBI) framework for ABM parameter estimation, SBI4ABM (Simulated-Based Inference 4 (for) ABM) Dyer et al. [2024] in a labour market ABM del Rio-Chanona et al. [2021]. By applying neural networks (NNs) and Bayesian theory, SBI4ABM can more effectively incorporate uncertainty quantification and prior knowledge.

Previous research has explored alternative approaches to parameter estimation in labour market ABMs. Examples include methods minimising the sum of squared errors (SSE) and the Covariance Matrix Adaptation Evolution Strategy (CMA-ES) Goudet et al. [2017]. Both approaches yield point estimates without accounting for uncertainty - another limitation that motivates the adoption of Bayesian frameworks such as the SBI4ABM.

The goal of this paper is to evaluate the capability of the SBI4ABM framework in handling computationally intensive and stochastic ABMs. More specifically, whether the posterior density distributions derived by SBI4ABM accurately place the original ABM parameters in high-density areas. This work also addresses the lack of analyses of NN-based tools applied to ABM parameter estimation Lux [2023], Avegliano and Sichman [2023].

1 ABM parameter estimation

Parameter estimation for stochastic ABMs poses significant computational challenges. As the labour market ABM analysed in this work, such ABMs present a large population of agents that might generate emergent behaviour through local interactions, requiring simulations that scale computationally with both agent count and interaction complexity Thiele et al. [2014], Broniec [2021]. Another challenge lies in high-dimensional parameter spaces. The combinatorial search of possible parameter ranges and combinations raises challenges that traditional optimisation methods struggle to navigate efficiently Bergman et al. [2024]. In addition, the stochasticity from probabilistic behavioural rules introduces statistical variability problems that necessitate extensive sensitivity analyses and repeated simulations to distinguish systemic patterns from noise Thiele et al. [2014], Monti et al. [2023].

1.1 Simulation-based inference for ABM parameter estimation

Simulation-based inference (SBI) is a likelihood-free inference technique extensively used for parameter estimation, particularly when direct computation of the likelihood function is infeasible Hashemi et al. [2023]. By performing extensive simulations across parameter sets, SBI approximates the posterior distribution $p(\boldsymbol{\theta}|\mathbf{y})$, the probability distribution over parameter values after seeing the data $\mathbf{y}$, making it especially suitable for ABMs Cranmer et al. [2020].

Summary statistics address the high dimensionality of ABM outputs. These summary statistics can either be handcrafted - a static list of statistical measures that require domain expertise and careful selection Cranmer et al. [2020] - or automatically learned from simulated data by constructing a separate learning module, usually a NN.

1.2 SBI4ABM

In this paper, we assess the performance of the SBI4ABM Dyer et al. [2024], a framework tailored for parameter estimation of high-dimensional models, such as ABMs applied to economic modelling. SBI4ABM addresses the limitations of traditional methods by integrating advanced machine learning techniques: the neural posterior estimation (NPE) Papamakarios and Murray [2016], Lueckmann et al. [2017], Greenberg et al. [2019] and the neural ratio estimation (NRE) Hermans et al. [2020]. NPE directly approximates the posterior density, and NRE approximates the likelihood-to-evidence ratio. The experiments described in later sections focus on the NPE.

In NPE, NNs are trained to approximate the global posterior density $p(\boldsymbol{\theta} \mid \mathbf{y})$ across all possible values of $\boldsymbol{\theta}$ and $\mathbf{y}$ using a limited number of simulations compared to methods such as Approximate Bayesian Computation (ABC). The training for a global density estimator benefits the NN-based methods with amortisation: once trained, the NN can generate many posterior samples without additional ABM simulations. NPE is implemented using normalising flows (NF), a machine learning model to transform a simple base distribution (e.g., Gaussian) into a complex one that closely matches the true posterior, via invertible transformations. The neural estimators incorporated into the SBI4ABM framework have been shown to outperform traditional methods in terms of the accuracy of estimated posterior distributions Dyer et al. [2024].

1.3 Labour Market Occupational Mobility and Automation ABM

The target ABM is the Labour Market Occupational Mobility and Automation ABM (LM-ABM) del Rio-Chanona et al. [2021]. This model simulates the effects of automation on workforce distribution in the U.S. It focuses on the mobility of employees between occupations of an out-of-equilibrium economy as the labour market adjusts to a new steady state after automation shocks.

We can describe a labour market as having $n \in \mathbb{N}$ occupations, a workforce distributed in those occupations $\mathbf{z} = [z_1, z_2, ..., z_n], \quad z_i \in \mathbb{N}$, the automation probability per occupation $\mathbf{p} = [p_1, p_2, ..., p_n], \quad p_i \in [0, 1]$, and a matrix of transition probabilities between different occupations $\mathbf{P_{i,j}} \in \mathbb{R}_{+}^{n \times n}$ where each element gives the probability of transitioning from occupation i to occupation j. For parameter estimation, an observed value of the labour market, $\mathbf{y} \in \mathbb{R}^n$, should also be provided.

During each discrete time step, t, for each occupation i, the ABM computes the economic indicators listed in Table 1.

Table 1: Economic indicators for occupation i at time t

Variable	Description
$e_{i,t}$	Number of employed workers
$u_{i,t}$	Number of unemployed workers last employed in occupation i
$v_{i,t}$	Number of job vacancies
$d_{i,t}$	Labour demand

Table 2: ABM Parameters

Parameters	Description
δ_u	Rate at which employed workers are separated (fired)
δ_v	Rate at which new vacancies are opened
r	Probability that a worker stays in the same occupation

The dynamics of the labour market are governed by shifts in labour demand, which depend on two processes: worker separation (firing) and vacancy creation. Worker separation occurs with rate δ_u, while vacancy creation happens with rate δ_v, contingent upon the number of currently employed workers in the same occupation. Let $r \in [0, 1]$ denote the probability that a worker remains in the same occupation each time step. These parameters are the same for all occupations and are presented in Table 2.

2 Methodology

Let the parameter vector of interest within the LM-ABM framework be denoted as in (1):

$$\theta = [\delta_u, \delta_v, r]. \tag{1}$$

This study employs SBI4ABM to estimate the parameters in (1) as they are fundamental determinants of labour market dynamics (detailed in Table 2).

Let the simulation be run for a maximum of T time steps. Each time step t generates a matrix $\mathbf{S}_t$ representing the ABM state: 4 economic indicators in Table 1 per n occupations. The LM-ABM output is defined as in (2):

$$\mathbf{X}_A = [\mathbf{S}_1 \quad \mathbf{S}_2 \quad \dots \quad \mathbf{S}_T], \qquad \mathbf{X}_A \in \mathbb{R}^{n \times 4T}. \tag{2}$$

In addition to economic indicators, we are also interested in applying SBI4ABM for parameter estimation using microdata Dyer et al. [2022]. Microdata in the context of LM-ABM refers to traces of workers' job transitions. To accommodate this, we adapted the LM-ABM to output a time series of job transition matrices, where at t, the matrix $\mathbf{J}_t = [J_{ij}]_t$ records the transitions of workers from occupation i to j. Combining job transition data (microdata) with occupation-specific economic conditions (aggregate macrodata), the final output matrix is defined in (3).

$$\mathbf{X}_B = [\mathbf{J}_1 \quad \mathbf{J}_2 \quad \dots \quad \mathbf{J}_T], \quad \mathbf{X}_B \in \mathbb{R}^{n \times (n+4) \times T}. \tag{3}$$

Initial experiments were conducted on synthetic datasets with fewer occupations than the complete U.S. dataset. This approach allowed for evaluating the impact of varying the number of occupations on the full SBI4ABM pipeline execution time and memory requirements Kissel and Diepold [2023]. To create the synthetic data, we defined which properties of the original U.S. dataset should be replicated. By considering the characteristics of the LM-ABM, we aimed to preserve the workforce's occupational composition and the stochastic properties of the transition matrix. In the synthetic data, labour force $\mathbf{z}$ is kept proportional to the number of occupations n. The automation probabilities $\mathbf{p}$ replicate values ranging from 0 to 0.9 in the original data. The transition probability matrix $\mathbf{P_{i,j}}$ was constructed using a modified version of the block-pattern algorithm with smoothing Behrisch et al. [2016].

2.1 Applying the SBI4ABM pipeline in the Labour Market ABM

The input of the SBI4ABM pipeline are: the initial conditions of the labour market, namely $\mathbf{P_{i,j}}$, $\mathbf{z}$, $\mathbf{p}$, the parameters to be estimated, $\boldsymbol{\theta}$, and their respective prior distributions and the number of simulations used to train the NN. For

Table 3: SBI4ABM arguments

Argument	Value
$\delta_{u_{true}}$	0.016
$\delta_{v_{true}}$	0.012
r_{true}	0.55
Range of δ_u	[0.0, 0.02]
Range of δ_v	[0.0, 0.02]
Range of r	[0.0, 1]

parameter estimation, a sample of empirical data from the phenomenon under investigation, $\mathbf{y}$, is needed. As we do not have a real time series of economic descriptors, we initially assume that the LM-ABM is correctly calibrated. To create a sample of empirical labour market data, the ABM is executed using known parameter values (the original parameters used in del Rio-Chanona et al. [2021]), which will be used in the inference phase. The ABM known parameter values and the explored prior distributions are listed in Table 3.

SBI4ABM starts by sampling parameter set values from the uniform prior distribution of $p(\boldsymbol{\theta})$ and uses those to generate ABM simulated data $\mathbf{x}$. The pairs $(\boldsymbol{\theta}, \mathbf{x})$ after the sampling and simulation phase form a dataset to train the NN density estimator. Encapsulated within an NPE class, the density estimator iteratively improves its approximation to the density via simulations. The conditional density estimator is based on the masked autoregressive flow (MAF), a normalising flow that incorporates autoregressive models as its core building blocks. The MAF-based approximation of NPE guides the parameter sampling for subsequent simulations, thereby refining the inference. After the training, the approximated posterior distribution is obtained by conditioning the posterior distribution on the observed data, $\mathbf{y}$, through the trained density estimator.

2.2 LM-ABM economic indicators

In the first phase of experimentation, we address dimensional compatibility and the computation of summary statistics within the SBI4ABM. We work with LM-ABM output represented as a multidimensional matrix of economic indicators (2). As SBI4ABM only processes second-order tensors, we apply a tensor reshaping function to enable compatibility $\phi : \mathbb{R}^{n\times 4\times T} \rightarrow \mathbb{R}^{d_1\times d_2}$ where d_1 corresponds to the focal analytical dimension of the simulation and d_2 represents the combination of the other 2 dimensions. Emphasising the dimension of time steps T, we transform the ABM output as such that $\mathbf{X_A} \in \mathbb{R}^{T\times(n\times 4)}$.

2.2.1 Dimensionality reduction

A common issue in parameter inference is selecting the method for data dimensionality reduction. A predefined handcrafted set of statistical measures to describe the data is usually applied to compare the model output, $\mathbf{x}$, and the real-world sample data, $\mathbf{y}$. In SBI4ABM, it is also possible to perform dimensionality reduction via learned summary statistics using an embedding NN. The resulting low-dimensional representations are directly provided to the conditional density estimator, without further transformation.

Using handcrafted statistics, for each row vector of the reshaped matrix $\mathbf{X_A} \in \mathbb{R}^{T\times(n\times 4)}$, we computed ten statistical measures: min, max, $\bar{x}$, σ^2, Q_p where p is the p-th quantile ($p = 0.25, 0.5, 0.75$), and ρ_k where k is the the autocorrelation at lag $k = 1, 2, 3$.

We create a synthetic labour market with $n = 10$ occupations and run the SBI4ABM pipeline with handcrafted statistics to estimate the LM-ABM parameters using the values listed in Table 3. The posterior distribution sampling and pairwise marginals are depicted in Fig. 1. True parameter values are indicated in orange.

The density plot in Fig. 1 accurately highlights the true parameter value of δ_u within a high-density region. Notably, the pairwise relationship between δ_u and δ_v emerged across all plots, a point that has not been listed in the original description of the LM-ABM in del Rio-Chanona et al. [2021].

For NN-learned summary statistics, we apply the SBI4ABM implementation of a Recurrent Neural Network (RNN) Chung et al. [2014]. Given the ABM output matrix, defined in (2), the RNN operates across T sequential steps with input size $n \times 4$. The resulting samples from the approximated posterior distribution and the pairwise marginals of a synthetic labour market with $n = 10$ occupations are shown in Fig. 2.

NN-learned summary statistics in Fig. 2 suggest improved precision in parameter estimation, showing more concentrated distributions and sharp peaks around the true parameter values. The pairwise marginals further confirm the tighter

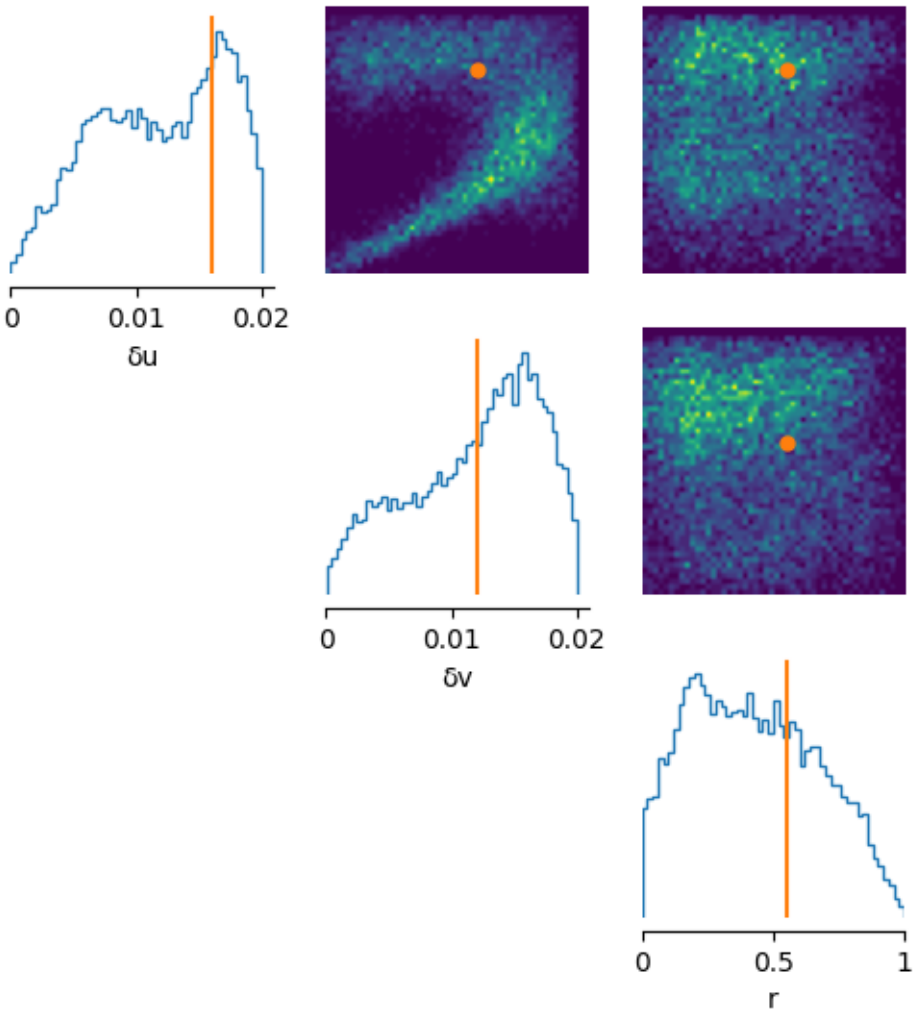

Figure 1: Sampling and pairwise marginals from an NPE trained with a list of statistic measures. Labour market with 10 synthetic occupations

concentration of inferred distributions. In contrast, the broader distributions of handcrafted statistics in Fig. 1 indicate high variability and noise, suggesting a less accurate representation of the parameter relationships. This is evidence that learning summary statistics might yield more reliable and informative posterior distributions than handcrafted ones. These results underscore the sensitivity of posterior estimation to the choice of summary statistics.

2.2.2 SBI4ABM scalability

Applying ABMs to real-world labour market scenarios requires processing large datasets containing hundreds of occupations and millions of workers. Therefore, we conducted the next experiments to assess the scalability of SBI4ABM in synthetic labour markets that approximate the scale of real-world labour market data.

The scalability of SBI4ABM, specifically with learned statistics, is fundamentally influenced by the dimensions of the ABM output representation, $\mathbf{X_A} \in \mathbb{R}^{T\times(n\times 4)}$, which, in turn, depends on the number of occupations. The SBI4ABM is applied to synthetic labour markets with the number of occupations n ranging from 10 to 460 (approximately the value of occupations in the U.S. labour market). We recorded the simulation and training times across 25 executions of the pipeline for each number of occupations. The average simulation time and average training time are depicted in Fig. 3 and Fig.4, respectively.

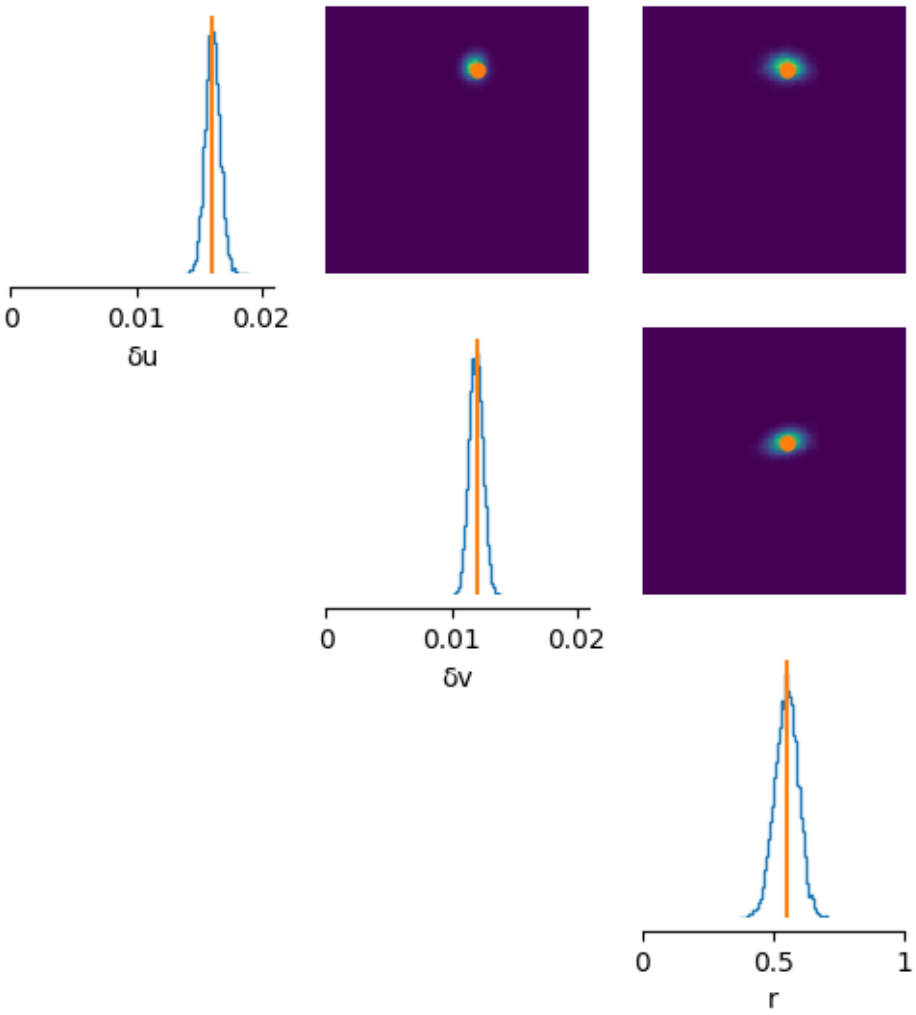

Figure 2: Sampling and pairwise marginals from an NPE trained with a NN-learned summary statistics. Labour market with 10 synthetic occupations

The averages in Fig. 3 show that the execution time is consistent for the same number of occupations, with a very low standard deviation, except for one anomaly. Although fast compared to other tasks in the parameter estimation pipeline, the simulation phase requires careful consideration of memory allocation for storing the high-dimensional ABM output.

Fig. 4 reveals that for $n > 360$, the plot exhibits high variability across all occupations outside the upper and lower quartiles. The smaller number of occupations, ranging from 10 to 135, exhibits relatively narrower variability compared to larger n. The training time becomes less consistent as the number of occupations increases. Factors contributing to this might include more complexity of occupation data and hardware resource constraints that become more pronounced with larger datasets. Training time is related to the number of epochs required for convergence. However, because the Pearson correlation coefficient between training time and the number of epochs is 0.93, the plot omits the number of epochs for clarity.

2.2.3 U.S. labour market

We executed the LM-ABM using U.S. data. $\mathbf{P_{i,j}}$ and $\mathbf{z}$ are originated from the Current Population Survey (2010–2017) available from the U.S. Bureau of Labour Statistics, and the automation probabilities $\mathbf{p}$ for U.S. occupations were extracted from del Rio-Chanona et al. [2021].

In the LM-ABM environment, a fiscal year comprises 52 weeks, where a single time step t corresponds to 6.75 weeks. The simulation is executed for $T = 600$ time steps, encompassing approximately 78 years of labour market dynamics

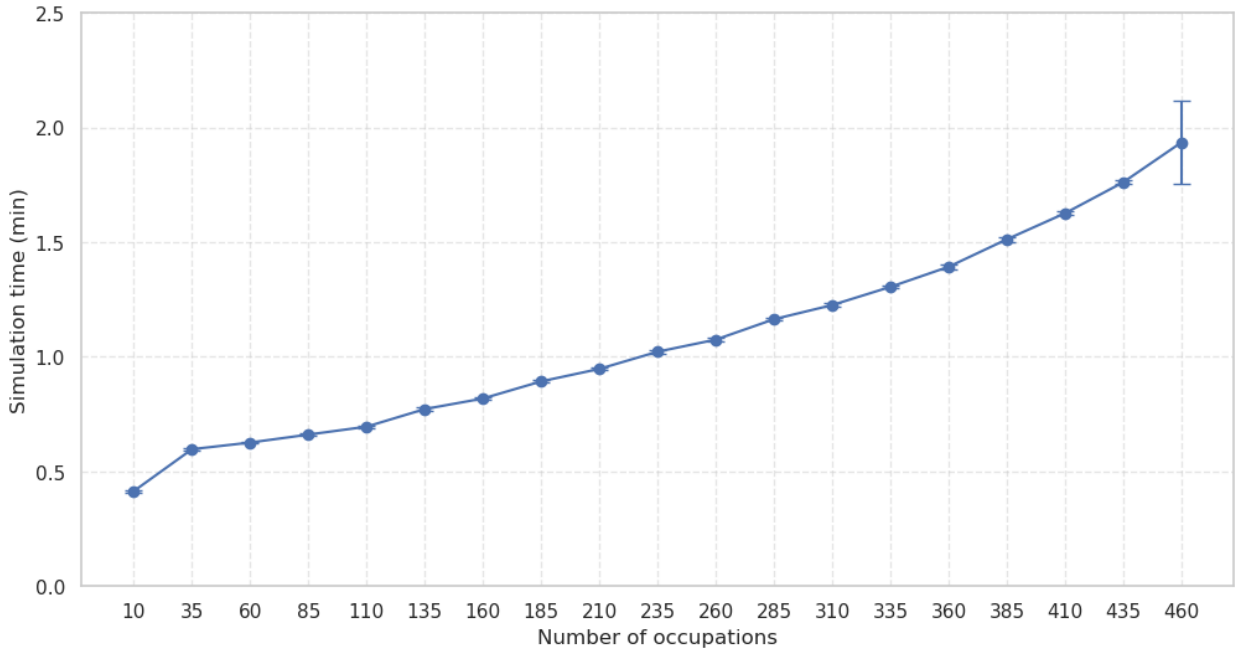

Figure 3: Average SBI4ABM simulation time per number of occupations

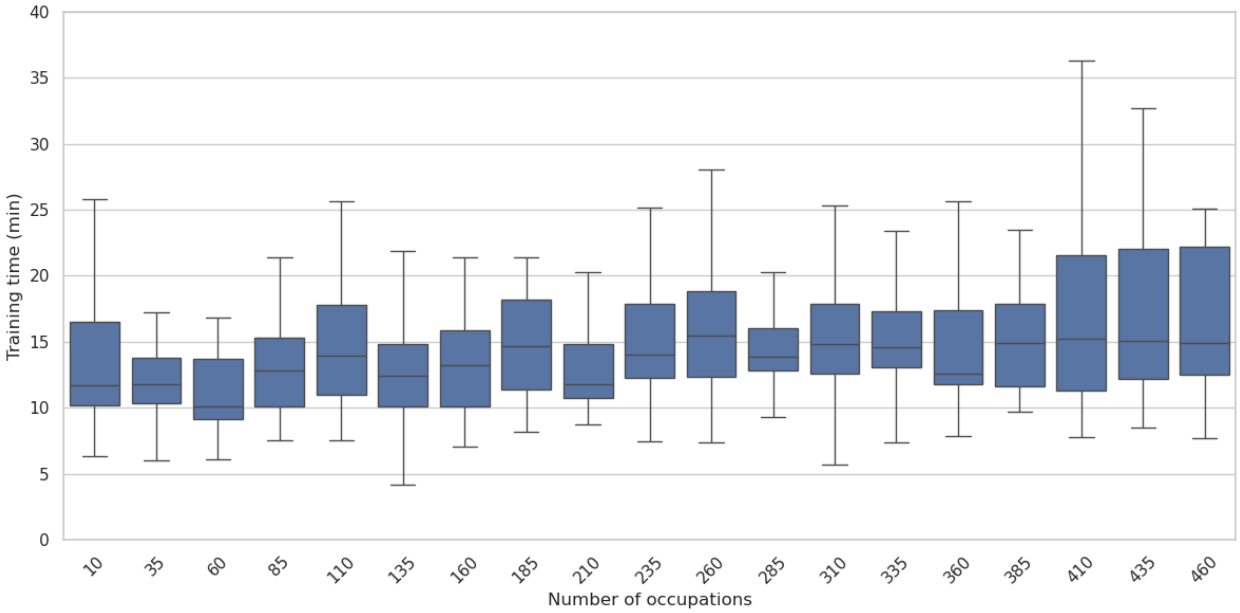

Figure 4: Average SBI4ABM training time per number of occupations

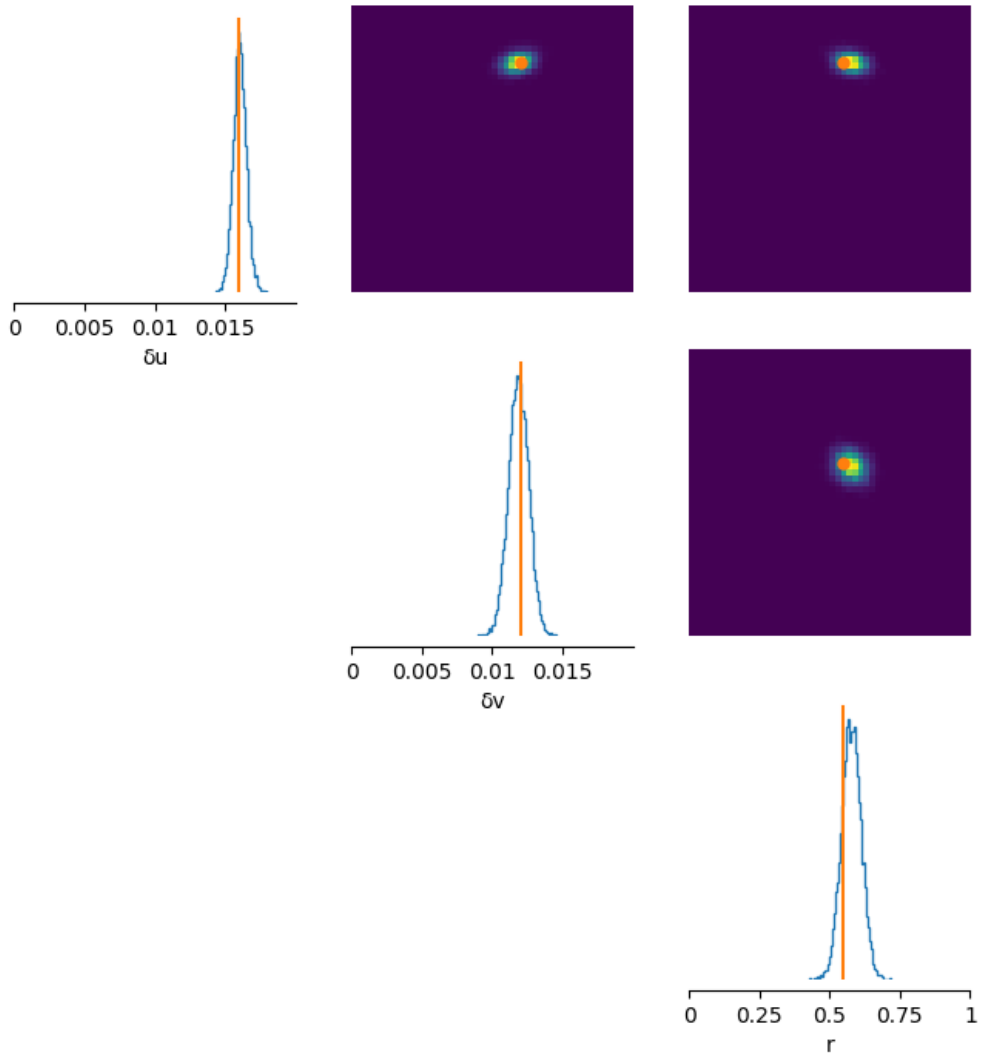

Figure 5: Sampling and pairwise marginals by learned summary statistics of the U.S. labour market

and incorporating an exogenous automation shock in 464 occupations at the 30-year mark. To enable parameter estimation of such a hypothetical scenario, a pseudo-real dataset $\mathbf{y}$ was generated from the model using the known parameter variable from del Rio-Chanona et al. [2021]. The samples from the posterior distribution and pairwise marginals are shown in Fig. 5.

Using the trained NPE posterior approximation for the U.S. labour market, we leverage posterior samples to compute their correlations and analyse parameter interdependencies. Additionally, we perform targeted sampling from high-density regions of the posterior distribution to analyse how the parameter configurations influence the LM-ABM dynamics. The outcomes are summarised in Fig. 6 and Fig. 7.

The posterior parameter correlation matrix for δ_u, δ_v, and r for the U.S. labour market is shown in Fig. 6. A weak positive correlation of 0.24 was observed between δ_u and δ_v, indicating limited interdependence between these parameters. The weak negative correlations of r with δ_u (-0.21) and δ_v (-0.19) imply a slight decrease in these unemployment and new vacancies as r increases. An increase in r could correspond to more workers continuing in their occupations when new vacancies open, but also to higher unemployment given the increase in demand after the automation shock.

Figure 7 presents the investigation of occupational labour market dynamics. In these experiments, we execute the LM-ABM with a fixed $r = 0.55$ parameter to analyse the interplay between employment and unemployment. From the regions with the highest posterior density in the posterior density estimator, 100 parameter sets were sampled.

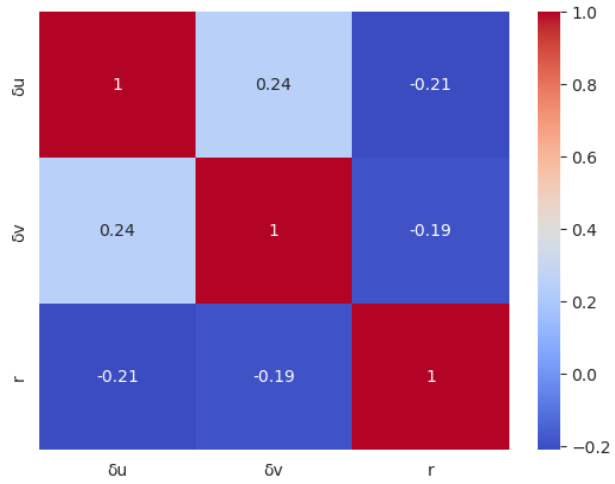

Figure 6: Posterior parameter correlation of δ_u, δ_v, and r

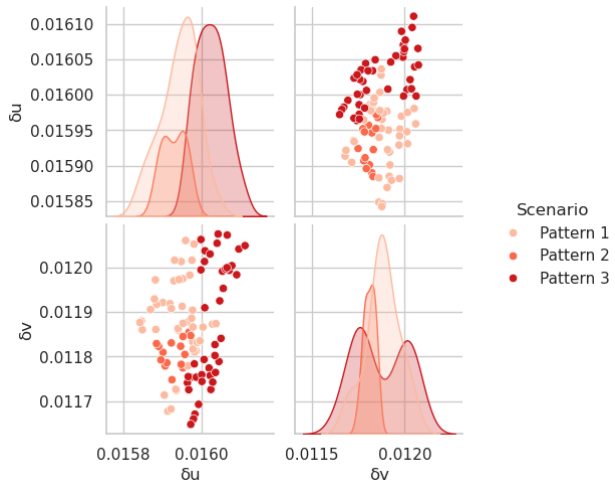

Figure 7: Identified patterns describing the relation between unemployment rate δ_u and new vacancies rate δ_v when the probability of a worker staying in the same occupation is constant $r = 0.55$ in multiple runs

Simulations were initialised with each one of these parameter sets, and the evolution of employment and unemployment was tracked over time. Analysis revealed three distinct patterns: Pattern 1, characterised by lower parameter values (both δ_u and δ_v), reflected greater stability with fewer such occurrences, and Pattern 2 occupied an intermediate transitional state. In contrast, Pattern 3 exhibits higher parameter values, signalling a more turbulent labour market in which job creation and job destruction occur more frequently and often in parallel. While Patterns 2 and 3 showed substantial overlap in δ_v distributions, Pattern 3 exhibited a stronger propensity for elevated unemployment. The groups are shown in Fig. 7; the darkest shades of red indicate the highest intensity of simultaneous gains and losses in employment. These groups indicate that even when employment rises within an occupation, automation shocks can exacerbate unemployment, influenced by the rates governing changes in employment and unemployment. In the labour market, this phenomenon may arise from the creation of new job categories or from demand for complementary skills, while skill mismatches and transitional labour market frictions can increase unemployment.

2.2.4 Validation of Bayesian inference with SBC

Simulation-based calibration (SBC) Talts et al. [2018] is a diagnostic tool for assessing Bayesian inference. It inspects whether the inference approach under test appropriately quantifies parameter uncertainty. Uniform rank histograms for

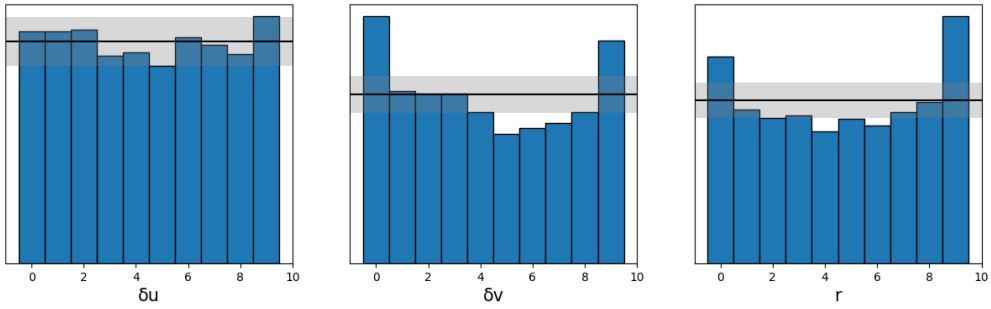

Figure 8: Ranks from a posterior estimator with handcrafted summary statistics. Synthetic labour market with $n = 10$ occupations

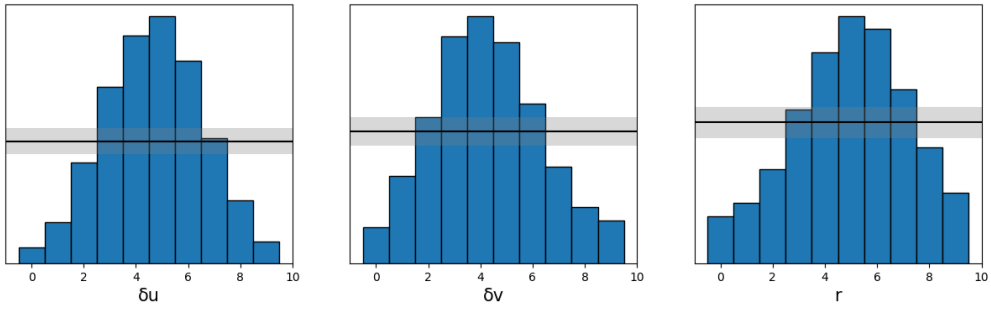

Figure 9: Ranks from a posterior estimator with handcrafted summary statistics. Synthetic labour market with $n = 10$ occupations

all components $\boldsymbol{\theta}$ are expected under proper calibration Talts et al. [2018]. Fig. 8 and 9 show the SBC results NPE trained with summary statistics by handcrafted and learned statistics, respectively.

Although the marginals and pairwise marginals derived from NPE with handcrafted summary statistics (Fig. 1) indicate a less accurate capture of the underlying parameter relationships, the associated rank plot (Fig. 8) exhibits the surprising finding of the most uniform distribution across all experiments. The grey region highlights the range within which 99% of the histogram bars would fall if the ranks were truly uniform, accounting for finite-sample variability. The distributions suggest that the estimator does not exhibit significant systematic biases. The absence of severe over- or under-representation of certain rank values indicates that the posterior inference is well-calibrated.

The marginals and pairwise marginals of NPE with embedded RNN (learned) demonstrate values converging closely to the true parameters as seen in Fig. 2. However, the corresponding rank plots in Fig. 9 show histograms with central peaks and under-represented tails. Such patterns imply that the NPE posterior is overly concentrated compared to the true posterior, leading to under-dispersed credible intervals. The rank histogram suggests that the learned summary statistics may either be insufficient to describe the ABM output time series, or that bias was introduced during dimensionality reduction.

2.3 LM-ABM as job transitions

In the context of LM-ABM, microdata refers to traces of actual job transitions during ABM execution. The result is a multidimensional matrix as shown in (3). The parameter estimation of ABMs using granular microdata, typical of real-world social systems, is driven by the increasing availability of detailed economic data Monti et al. [2023]. However, despite the availability and volume of data, existing SBI methods often struggle to accommodate the dynamic graph structures inherent in fully observed ABMs and their associated datasets Dyer et al. [2022].

Fully observed ABMs generate exceptionally large datasets. For instance, in the LM-ABM setting, calculating memory requirements for `float16` matrices with dimensions $1000 \times 600 \times 464 \times 468$ yields $130,636,800,000$ elements, requiring approximately 243.34 GB of storage. This exceeds the standard memory capacity (experiments run on a Ubuntu PowerEdge R760XA Server) and requires adaptation measures, such as reducing the simulation length or simplifying the model. While the SBI4ABM framework demonstrated high efficiency in the number of simulations,

testing was limited by memory constraints. The NN training phase further exacerbates these limitations, as it requires substantial memory resources that prevent successful execution. Even under a constrained configuration in which the ABM was executed for 430 time steps, and simulations were reduced to 500 runs, the simulation phase alone required approximately 90 GB of memory. This left insufficient RAM for subsequent training phases, further underscoring the substantial memory demands of this computational pipeline. Due to these limitations, experiments using U.S. labour market data were infeasible.

3 Conclusion

This study applied and evaluated the SBI4ABM pipeline for parameter estimation of a labour market ABM. By applying synthetic data and data from the U.S. labour market, our experiments revealed three critical insights: firstly, the scalability of the pipeline with duration scaling linearly with occupation count, which demonstrates the applicability of the framework for real-world size models; secondly, the statistical comparison showed that learned statistics yielded sharper posterior distributions than handcrafted alternatives but exhibited validation issues emphasising the trade-off between precision and reliability; and thirdly, limitations of the pipeline when dealing with microdata.

We recognise that the current study is subject to limitations. The synthetic data generation is based on a simplistic algorithm. While the synthetic data proved useful for experiments focused on processing time, it only captured basic distributions of workers across occupations and job transition probabilities. Additionally, the absence of real-world job transition data constrained validation efforts to compare the ABM output with the U.S. labour market.

These findings highlight the potential of SBI4ABM and NN-based Bayesian frameworks to advance ABMs from experimental "toy models" to decision-making tools. However, challenges persist in real-world data integration and model validation. Future research should focus on architectural optimisations for summary statistic networks and on incorporating longitudinal real-world data.

References

Joshua C. Jackson, David Rand, Kevin Lewis, Michael I. Norton, and Kurt Gray. Agent-based modeling: A guide for social psychologists. *Social Psychological and Personality Science*, 8(4):387–395, 2017.

Pedro C. L. Silva, Paulo V. C. Batista, Hugo S. Lima, Marcos A. Alves, Frederico G. Guimarães, and Rodrigo C. P. Silva. Covid-abs: An agent-based model of covid-19 epidemic to simulate health and economic effects of social distancing interventions. *Chaos, Solitons & Fractals*, 139:110088, 2020. doi:10.1016/j.chaos.2020.110088.

James Dyer, Patrick Cannon, J. Doyne Farmer, and Sebastian M. Schmon. Black-box bayesian inference for agent-based models. *Journal of Economic Dynamics and Control*, page 104827, 2024.

R. M. del Rio-Chanona, Penny Mealy, Mariana Beguerisse-Díaz, Francois Lafond, and J. Doyne Farmer. Occupational mobility and automation: A data-driven network model. *Journal of The Royal Society Interface*, 18(174):20200898, 2021.

Olivier Goudet, Jean-Daniel Kant, and Gérard Ballot. Worksim: A calibrated agent-based model of the labor market accounting for workers' stocks and gross flows. *Computational Economics*, 50:21–68, 2017.

Thomas Lux. Approximate bayesian inference for agent-based models in economics: A case study. *Studies in Nonlinear Dynamics & Econometrics*, 27(4):423–447, 2023.

Pablo Avegliano and Jaime S. Sichman. Equation-based versus agent-based models: Why not embrace both for an efficient parameter calibration? *Journal of Artificial Societies and Social Simulation*, 26(4):3, 2023.

Jan C. Thiele, Winfried Kurth, and Volker Grimm. Facilitating parameter estimation and sensitivity analysis of agent-based models: A cookbook using netlogo and r. *Journal of Artificial Societies and Social Simulation*, 17(3):11, 2014.

Wojciech Broniec. Guiding parameter estimation of agent-based modeling through knowledge-based function approximation. In *Proceedings of the AAAI 2021 Spring Symposium on Combining Machine Learning and Knowledge Engineering (AAAI-MAKE)*, 2021.

David R. Bergman, K.-A. Norton, H. V. Jain, and Thomas Jackson. Connecting agent-based models with high-dimensional parameter spaces to multidimensional data using smore pars: A surrogate modeling approach. *Bulletin of Mathematical Biology*, 86(1):11, 2024.

Corrado Monti, Marco Pangallo, Gianmarco De Francisci Morales, and Francesco Bonchi. On learning agent-based models from data. *Scientific Reports*, 13:9268, 2023.

M. Hashemi et al. Amortized bayesian inference on generative dynamical network models of epilepsy using deep neural density estimators. *Neural Networks*, 163:178–194, 2023.

Kyle Cranmer, Johann Brehmer, and Gilles Louppe. The frontier of simulation-based inference. *Proceedings of the National Academy of Sciences*, 117(48):30055–30062, 2020.

George Papamakarios and Iain Murray. Fast ε-free inference of simulation models with bayesian conditional density estimation. In *Advances in Neural Information Processing Systems*, volume 29, 2016.

Jan-Matthis Lueckmann et al. Flexible statistical inference for mechanistic models of neural dynamics. In *Advances in Neural Information Processing Systems*, volume 30, 2017.

David Greenberg, Marcel Nonnenmacher, and Jakob Macke. Automatic posterior transformation for likelihood-free inference. In *Proceedings of the International Conference on Machine Learning (ICML)*, pages 2404–2414. PMLR, 2019.

Joeri Hermans, Vladimir Begy, and Gilles Louppe. Likelihood-free mcmc with amortized approximate ratio estimators. In *Proceedings of the International Conference on Machine Learning (ICML)*, pages 4239–4248. PMLR, 2020.

James Dyer, Patrick Cannon, J. Doyne Farmer, and Sebastian M. Schmon. Calibrating agent-based models to microdata with graph neural networks. ICML 2022 Workshop on Artificial Intelligence for Agent-Based Modelling (Spotlight Paper), 2022. arXiv:2206.07570.

Maximilian Kissel and Klaus Diepold. Structured matrices and their application in neural networks: A survey. *New Generation Computing*, 41(3):697–722, 2023.

Michael Behrisch, Benjamin Bach, Nathalie H. Riche, Tobias Schreck, and Jean-Daniel Fekete. Matrix reordering methods for table and network visualization. *Computer Graphics Forum*, 35(3):693–716, 2016.

Junyoung Chung, Caglar Gulcehre, Kyunghyun Cho, and Yoshua Bengio. Empirical evaluation of gated recurrent neural networks on sequence modeling. NIPS 2014 Deep Learning and Representation Learning Workshop, 2014. arXiv:1412.3555.

Sean Talts, Michael Betancourt, Daniel Simpson, Aki Vehtari, and Andrew Gelman. Validating bayesian inference algorithms with simulation-based calibration. *arXiv preprint arXiv:1804.06788*, 2018.